*J Physiol* 590.7 (2012) pp 1655–1667



The Journal of Physiology

# Opioid-related (ORL1) receptors are enriched in a subpopulation of sensory neurons and prolonged activation produces no functional loss of surface N-type calcium channels

Swetha S. Murali, Ian A. Napier, Beth K. Rycroft and MacDonald J. Christie

*Discipline of Pharmacology, University of Sydney, Sydney, NSW 2006, Australia*

**Key points**

- The nociceptin/ORL1 receptor neuropeptide system is related to opioid systems and thought to be involved in pain modulation.
- A major mechanism of action of this system is inhibition of calcium channels that control excitability of sensory nerves.
- To understand the potential for drugs acting on this system to modulate pain it is important to identify the types of sensory nerve cells functionally expressing the ORL1 receptor and how they are modulated.
- Here we identified a subpopulation of small, presumably pain sensing sensory nerves that are highly responsive to this neuropeptide both in their cell bodies and nerve terminals.
- We then established that nociceptin/ORL1 stimulation inhibits calcium channels only while the peptide is present on the cells or their nerve terminals but does not produce long-term down-regulation of calcium channel function as had been previously proposed.

**Abstract** The opioid-related receptor, ORL1, is activated by the neuropeptide nociceptin/orphanin FQ (N/OFQ) and inhibits high-voltage-activated (HVA) calcium channel currents ($I_{Ca}$) via a G-protein-coupled mechanism. Endocytosis of ORL1 receptor during prolonged N/OFQ exposure was proposed to cause N-type voltage-gated calcium channel (VGCC) internalization via physical interaction between ORL1 and the N-type channel. However, there is no direct electrophysiological evidence for this mechanism in dorsal root ganglion (DRG) neurons or their central nerve terminals. The present study tested this using whole-cell patch-clamp recordings of HVA $I_{Ca}$ in rat DRG neurons and primary afferent excitatory synaptic currents (eEPSCs) in spinal cord slices. DRG neurons were classified on the basis of diameter, isolectin-B4 (IB4) binding and responses to capsaicin, N/OFQ and a $\mu$-opioid agonist, DAMGO. IB4-negative neurons less than 20 $\mu$m diameter were selectively responsive to N/OFQ as well as DAMGO. In these neurons, ORL1 desensitization by a supramaximal concentration of N/OFQ was not followed by a decrease in HVA $I_{Ca}$ current density or proportion of whole-cell HVA $I_{Ca}$ contributed by N-type VGCC as determined using the N-type channel selective blocker, $\omega$-conotoxin CVID. There was also no decrease in the proportion of N-type $I_{Ca}$ when neurons were incubated at 37°C with N/OFQ for 30 min prior to recording. In spinal cord slices, N/OFQ consistently inhibited eEPSCs onto dorsal horn neurons. As observed in DRG neurons, preincubation of slices in N/OFQ for 30 min produced no decrease in the proportion of eEPSCs inhibited by CVID. In conclusion, no internalization of the N-type VGCC occurs in



DOI: 10.1113/jphysiol.2012.228429

either the soma or central nerve terminals of DRG neurons following prolonged exposure to high, desensitizing concentrations of N/OFQ.

(Received 17 January 2012; accepted after revision 20 February 2012; first published online 27 February 2012)
**Corresponding author** M. J. Christie: Discipline of Pharmacology, Blackburn Building D06, University of Sydney, Sydney, NSW 2006, Australia. Email: mac.christie@sydney.edu.au

**Abbreviations** BSA, bovine serum albumin; CVID, $\omega$-conotoxin CVID; DAMGO, [Tyr-D-Ala-Gly-MePhe-Gly-ol]enkephalin; DRG, dorsal root ganglion; ORL1R, opioid receptor-like receptor 1; N/OFQ, nociceptin/orphanin FQ; HBS, Hepes-buffered saline; HVA, high-voltage activated; IB4, isolectin B4; ME, [Met$^5$]-enkephalin; MOR, $\mu$-opioid receptor; TRPV1, transient receptor potential channel subfamily V member 1; VGCC, voltage-gated calcium channel.

## Introduction

The opioid-like receptor, ORL1, and its endogenous ligand, nociceptin/orphanin FQ (N/OFQ) comprise a signalling system closely related to, but distinct from, opioid systems (Meunier *et al.* 1995; Reinscheid *et al.* 1995). Activation of the ORL1 receptor (ORL1R) couples to G-protein-related signalling mechanisms including inhibition of VGCCs and activation of $K^+$ channels (Connor *et al.* 1996*a*,*b*; Larsson *et al.* 2000; Borgland *et al.* 2001). Drugs that act on ORL1Rs have been implicated as potential therapeutics for several conditions, including pain (Reiss *et al.* 2008; Hayashi *et al.* 2010). The involvement of N/OFQ and the ORL1R in pain modulation is complex and activation of the ORL1R has been implicated in both analgesia and hyperalgesia (Courteix *et al.* 2004; Okuda-Ashitaka *et al.* 2006; Chen & Sommer, 2007). This is dependent on the distribution of the receptor; for example, intrathecal administration of N/OFQ is antinociceptive (Yamamoto *et al.* 1997) whilst intracerebroventricular injection appears to be pronociceptive (Meunier *et al.* 1995; Reinscheid *et al.* 1995).

The ORL1R is expressed by sensory neurons but little is known about the expression patterns and selective actions on specific, potentially nociceptive sub-populations. Studies in rat using *in situ* hybridisation have reported that ORL1R mRNA is expressed mainly in medium- to large-sized rat dorsal root ganglion (DRG) neurons (Pettersson *et al.* 2002). However, in rat DRG neurons, N/OFQ selectively inhibited high voltage-activated (HVA) calcium channel currents ($I_{Ca}$) in the majority of small- to medium-sized neurons ($<25$ $\mu$m diameter) but only in a small proportion of larger neurons (Beedle *et al.* 2004). Similarly, in mouse trigeminal ganglion neurons both N/OFQ and the $\mu$-opioid receptor (MOR) agonist DAMGO selectively inhibited HVA $I_{Ca}$ (predominantly $Ca_v2.2$) in a large proportion ($>80\%$) of small nociceptive neurons that did not express low-voltage-activated $I_{Ca}$ (Borgland *et al.* 2001). To study mechanisms of antinociceptive actions of N/OFQ in rat spinal cord, we first sought to identify whether functional expression of ORL1Rs was enriched in a subpopulation of rat DRG neurons as well as their terminals in the dorsal horn of spinal cord using patch-clamp electrophysiology in acutely isolated neurons and brain slices. We found that ORL1R coupling to inhibition of HVA $I_{Ca}$ was very selective for a subpopulation of small ($<20$ $\mu$m diameter) rat DRG neurons that are isolectin-B4 (IB4) -negative and, therefore, presumably peptidergic (Wang *et al.* 1994). Most of these neurons were also sensitive to DAMGO. Activation of the ORL1R also produced greater inhibition of primary afferent electrically evoked post-synaptic currents (eEPSCs) in lamina I of the superficial dorsal horn of the spinal cord, where small peptidergic fibres selectively terminate than in lamina $II_{inner}$ where nociceptive, IB4-positive fibres predominantly terminate (Braz *et al.* 2005). These findings provide a functional anatomical basis for antinociceptive actions of N/OFQ in spinal cord.

Prolonged agonist stimulation has been reported to desensitize (Connor *et al.* 1996*a*; Spampinato *et al.* 2002) and internalize the ORL1R (Spampinato *et al.* 2001, 2002; Corbani *et al.* 2004). A novel mechanism of modulation of ORL1R signalling was more recently proposed that involves co-internalisation of the ORL1R and the VGCC $\alpha$1-subunit, $Ca_v2.2$ (Altier *et al.* 2006). Altier *et al.* (2006) reported profound co-internalisation of ORL1Rs and $Ca_v2.2$ after exposure to N/OFQ for up to 30 min when these were heterologously expressed in cell lines. Due to a physical interaction between the C-termini of the ORL1R and $Ca_v2.2$ (Beedle *et al.* 2004), it was reported that co-internalisation leads to trafficking and degradation of $Ca_v2.2$ in lysosomes, thereby decreasing the membrane expression of $Ca_v2.2$ (Beedle *et al.* 2004; Altier *et al.* 2006). If present in sensory neurons, this mechanism would be expected to reduce excitability and transmitter release, thereby potentially producing antinociception. However, these studies (Altier *et al.* 2006) were performed mostly in cultured cells heterologously expressing ORL1R and $Ca_v2.2$ constructs. Only indirect, calcium imaging evidence for modulation in sensory neurons was provided to suggest that this phenomenon may occur *in vivo* (Altier *et al.* 2006). A more recent study further suggested that hetero-oligomers of ORL1 and MOR form when heterologously expressed in cell lines, and that activation

of either receptor could drive internalization of $Ca_v2.2$ (Evans *et al.* 2010).

Having identified a subpopulation of sensory neurons that very selectively express strong coupling of the ORL1R to $Ca_v2.2$, we sought to determine whether prolonged exposure of sensory neurons to a high desensitising concentration of N/OFQ could reduce $Ca_v2.2$ currents in small IB4-negative neurons or their nerve terminals. Although exposure to N/OFQ reliably desensitized ORL1R coupling to VGCC currents, prolonged incubation of DRGs in a supramaximal concentration of N/OFQ, or ORL1 plus MOR agonists, had no effect on HVA $I_{Ca}$ density or the proportion of HVA $I_{Ca}$ sensitive to the highly selective $Ca_v2.2$ blocker, $\omega$-conotoxin CVID (Lewis *et al.* 2000, 2012). Consistent with the results from DRG neurons, prolonged exposure to N/OFQ had no effect on the sensitivity of primary afferent eEPSCs onto lamina I or lamina $II_{inner}$ dorsal horn neurons to inhibition by CVID. Together, these results suggest that sustained activation of the ORL1R does not down-regulate $Ca_v2.2$ expression on the soma or nerve terminals of primary afferent neurons.

## Methods

Sprague–Dawley rats (3- to 7-week-old males ($n = 48$) for DRG recordings and 16- to 31-day-old males and females for spinal cord recordings ($n = 41$)) were used in this study. Animals were housed in groups of two to four with environmental enrichment on a 12 h/12h light–dark cycle at 22 ± 2°C, with *ad libitum* access to food and water. All experiments were conducted according to protocols approved by the Animals Ethics Committee of the University of Sydney, Sydney, NSW, Australia, which complies with the National Health and Medical Research Council 'Australian code of practice for the care and use of animals for scientific purposes'.

### Isolated DRG neuron preparation

Rats were anaesthetized with isofluorane (4% in air) and decapitated. Dorsal root ganglia (spinal levels L3–L5) were removed and placed in ice-cold Hepes-buffered saline (HBS) containing (mM): NaCl, 154; KCl, 2.5; $CaCl_2$, 2.5; $MgCl_2$, 1.5; Hepes, 10; glucose, 10; pH 7.2 (NaOH), 330 ± 5 mosmol $l^{-1}$. Cells were prepared using the methods outlined in Borgland *et al.* (2001). Briefly, ganglia were cut up with iridectomy scissors and incubated at 37°C for 15 min in oxygenated HBS containing 3 mg $ml^{-1}$ collagenase and for 25 min in oxygenated HBS containing 1 mg $ml^{-1}$ papain. The digestion was terminated with addition of HBS containing 1 mg $ml^{-1}$ bovine serum albumin (BSA) and 1 mg $ml^{-1}$ trypsin inhibitor. Ganglia were washed free of enzyme and enzyme inhibitors with room-temperature HBS. Cells were dispersed by gentle trituration through decreasing bore, silanized Pasteur pipettes with fire-polished tips. The cells were plated onto plastic culture dishes and kept at room temperature in HBS. Cells remained viable for up to 10 h after dissociation.

### Spinal cord slice preparation

Rats were anaesthetized with isofluorane (4% in air), decapitated and the lumbar region of the spinal cord was removed as previously described (Rycroft *et al.* 2007; Vikman *et al.* 2008). Transverse spinal cord slices (350 $\mu$m) were cut on a vibratome (Leica, VT1000) in an ice-cold solution of the following composition (mM): 100 sucrose, 63 NaCl, 2.5 KCl, 1.2 $NaH_2PO_4$, 1.2 $MgCl_2$, 2.4 $CaCl_2$, 25 glucose and 2.5 $NaHCO_3$. Slices were maintained at 32°C in a submerged chamber containing physiological saline solution (ACSF) consisting of (mM): 125 NaCl, 2.5 KCl, 1.2 $NaH_2PO_4$, 1.2 $MgCl_2$, 2.4 $CaCl_2$, 25 glucose and 2.5 $NaHCO_3$ (pH 7.4, osmolarity 305–310 mosmol $l^{-1}$), which was equilibrated with 95% $O_2$ and 5% $CO_2$. The slices were then transferred to a recording chamber and superfused continuously (2 ml $min^{-1}$) with ACSF. Experiments were performed at 32°C.

### Visualization of IB4 binding

Isolated DRG cells were pre-treated with 1 $\mu$g $ml^{-1}$ Alexa Fluor 488-conjugated *Bandeiraea simplicifolia* IB4 (Invitrogen) for 10 min at 22–24°C as previously described (Borgland *et al.* 2001). Neurons were washed with HBS for 5 min before fluorescence was examined on the inverted microscope (Olympus, IX50) used for patch-clamp recordings.

### Electrophysiological recording from DRG neurons

Ionic currents from rat DRG neurons were recorded in the whole-cell configuration of the patch-clamp method at room temperature (22–24°C). Dishes were continually perfused with HBS. For isolating $I_{Ca}$, the extracellular solution contained (mM): 140 tetraethylammonium chloride (TEACl), 2.5 CsCl, 2.5 $CaCl_2$, 10 Hepes, 1 $MgCl_2$, 10 glucose; pH 7.2 (CsOH), 330 ± 5 mosmol $l^{-1}$. The intracellular pipette solution contained (mM): 120 CsCl, 10 Hepes, 10 EGTA, 2 $CaCl_2$, 5 MgATP, 0.2 $Na_2GTP$, 5 NaCl; pH 7.3 (CsOH), 285 ± 5 mosmol $l^{-1}$. Recordings were made using an EPC-9 patch-clamp amplifier and corresponding PULSE software from HEKA Electronik (Lambrecht/Pfalz, Germany). Currents were sampled at 20–50 kHz and recorded on hard disk for later analysis. Patch pipettes were pulled from borosilicate glass (AM Systems, Everett, WA, USA). The pipette input resistance ranged between 1.5 and 2.5 MΩ. The capacitance of

individual cells was estimated by PULSE software by fitting an exponential to current responses to small rectangular voltage pulses and ranged between 10 and 50 pF. Series resistance was between 3 and 10 MΩ. Series resistance compensation of between 70% and 80% was used in all experiments. Capacitance transients were compensated automatically using a built-in procedure of the HEKA amplifier. Leak current was subtracted online using a *P*/8 protocol. Liquid junction potential of 4 mV was not corrected for.

Cell diameter was estimated from membrane capacitance measurement derived by PULSE software from the voltage-clamp charging curve. As previously reported (Borgland *et al.* 2001), directly visualized diameter (using a micrometer graticule) was highly correlated with diameter calculated from cell capacitance using the relationship in Borgland et al. (2001) assuming a specific membrane capacitance of 0.9 $\mu$F cm$^{-2}$. All cell diameter data are reported from the latter.

Peak HVA $I_{Ca}$ in each cell was determined by stepping the membrane potential from a holding potential of –90 mV to between –60 and 30 mV, for 10 ms, in 10 mV increments. Following this procedure, the test current was evoked (–80 to 0 mV) every 30 s and monitored for current stability before drugs were applied.

Cells were exposed to drugs via a series of flow pipes positioned above the cells. The inhibition by drugs was quantified by measuring the current isochronically from the peak of the control current in the presence and absence of the drug.

### Electrophysiological recording from spinal cord slices

Lamina I was visualised using infra-red Nomarski optics and presumed NK1-positive neurons were selected for experiments based on size and shape of the cell soma (Rycroft *et al.* 2007). Lamina II was identified as the translucent area adjacent to lamina I. Dorsal cells in this region were considered in lamina IIo and those ventral and adjacent to the less translucent lamina III considered lamina IIi. Whole-cell voltage-clamp recordings (holding potential –74 mV) of synaptic currents were made using a Digidata 1322A and a Multiclamp 700B amplifier (both from Molecular Devices, CA, USA). Patch electrodes with a resistance of 2–4 MΩ were filled with a solution consisting of the following (mM): 113 caesium gluconate, 10 EGTA, 10 Hepes, 17.5 CsCl, 8 $NaCl_2$, 3 QX-314, 2 MgATP and 0.3 NaGTP, plus 0.2% (w/v) biocytin; pH 7.2; osmolarity, 280–290 mosmol l$^{-1}$). Series resistance ($\leq$15 MΩ) was compensated by 80% and continuously monitored during experiments. Liquid junction potentials of –14 mV were not corrected for. Recordings were low-pass filtered at 4–6 kHz, sampled at 10 kHz and analysed off-line using Axograph X (Axograph Scientific, Australia). A bipolar tungsten electrode (FHC, ME, USA) was carefully placed in the dorsal root entry zone to ensure stimulation of primary afferent terminals and electrically evoked excitatory postsynaptic currents (eEPSCs) were recorded (0.01 Hz, 2–30 V, 100 $\mu$s). To isolate eEPSCs, all experiments were performed in the presence of strychnine (5 $\mu$M) and picrotoxin (100 $\mu$M) to block glycine- and $GABA_A$-mediated synaptic currents. Unless otherwise stated, eEPSCs were quantified by averaging a minimum of 20 consecutive responses for each condition. Only evoked currents with a clear first peak and no latency jitter were measured and included in the analysis to avoid contamination from polysynaptic events.

### Data analysis

All data are expressed as the mean ± SEM unless otherwise indicated. Concentration–response data were pooled for each group and fitted to a logistic equation with a minimum constrained to zero using the software package GraphPad Prism v. 3. Where noted, significant differences between means were tested using paired or unpaired two-tailed Student's *t* tests, or when more than two groups were included, one-factor ANOVA, followed by Dunnett's test. Differences between frequency data were tested using $\chi^2$ tests.

### Drugs and chemicals

DAMGO ([Tyr-D-Ala-Gly-MePhe-Gly-ol]enkephalin), [Met$^5$]-enkephalin, N/OFQ (Phe-Gly-Gly-Phe-Thr-Gly-Ala-Arg-Lys-Ser-Ala-Arg-Lys-Leu-Ala-Asn-Gln), bovine serum albumin, trypsin inhibitor (chicken egg white ovomucoid, Type II-O) and $CdCl_2$ were from Sigma-Aldrich. $\omega$-Conotoxin CVID was provided by R. J. Lewis, Institute of Molecular Biology, University of Queensland. Capsaicin was from Tocris Cookson (Bristol, UK). Papain and collagenase were from Worthington Biochemical Corporation (Freehold, NJ, USA). Alexa Fluor 488-conjugated IB4 was from Invitrogen.

## Results

### Categorization of rat DRG neurons

Rat DRG neurons were categorised on the basis of several criteria in order to identify whether or not a defined subpopulation of DRG neurons selectively responds to N/OFQ (Fig. 1). The criteria correlated with responses to a supramaximal concentration (see below) of N/OFQ (300 nM, Fig. 1*C*, *E*, *F* and *G*) included soma diameter (Fig. 1*F* and *G*), whether or not they were IB4-negative (presumed peptidergic) or IB4-positive (presumed non-peptidergic) using pre-incubation with

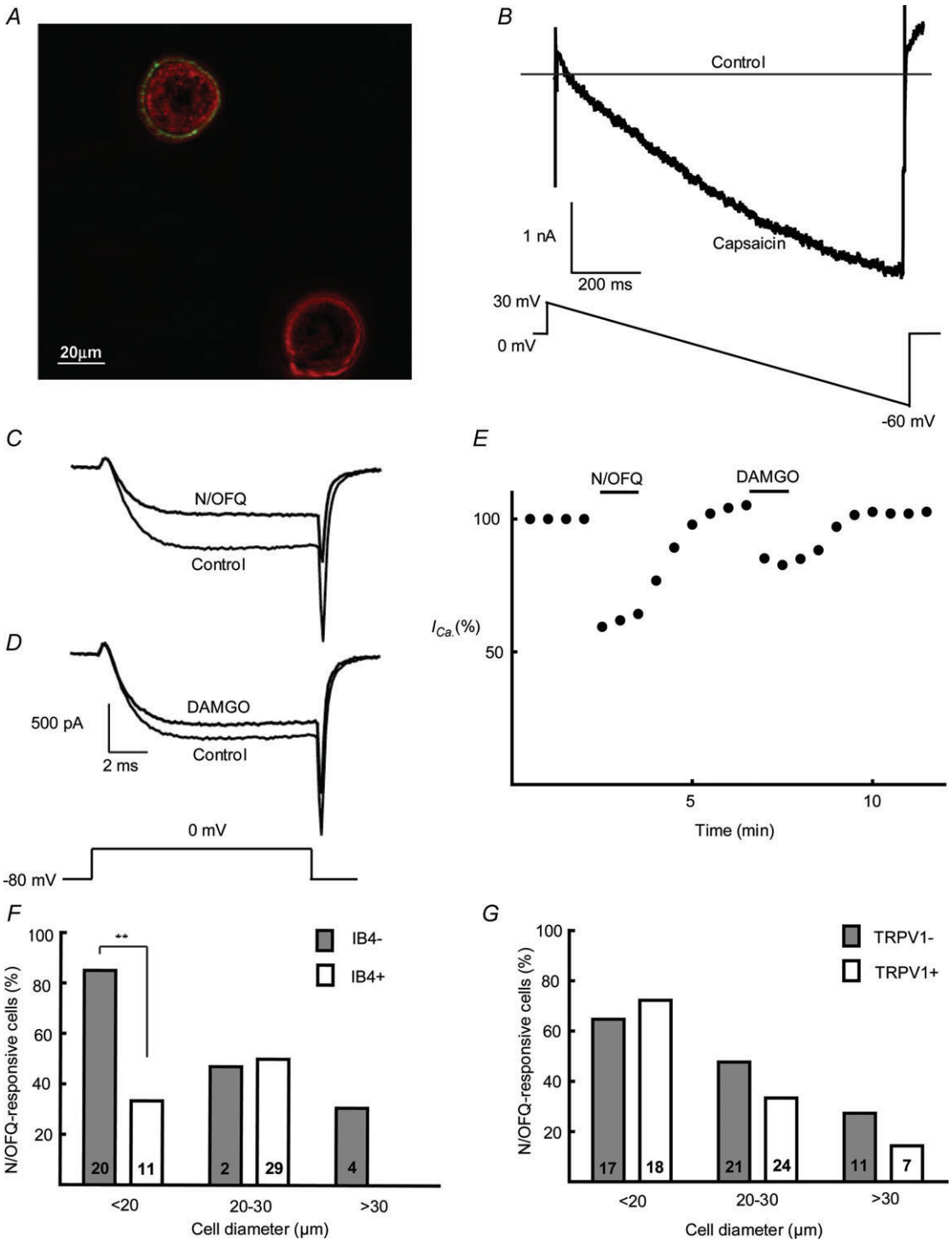


**Figure 1. Characterisation of DRG neuron phenotypes**
*A*, representative example of living DRG neurons exhibiting IB4 binding. The neuron at the top left is IB4$^+$ (non-peptidergic) while the other is IB4$^-$ (peptidergic). *B*, representative current trace from a TRPV1$^+$ neuron in the presence and absence of capsaicin (500 nM) during a continuous ramp from +30 mV to –60 mV of 1 s in duration. *C* and *D*, representative high-voltage-activated $I_{Ca}$ before and after application of N/OFQ (300 nM) and DAMGO (1 $\mu$M). *E*, $I_{Ca}$ amplitude as a percentage of total HVA $I_{Ca}$ indicating inhibition and recovery from N/OFQ (300 nM) and DAMGO (1 $\mu$M). *F* and *G*, percentage of neurons responsive to N/OFQ when categorised on the basis of size, IB4 binding and responsiveness to capsaicin (TRPV1$^+$ or $^-$). Note that 85% of IB4$^-$ neurons with soma diameter smaller than 20 $\mu$m are responsive to N/OFQ ($P = 0.003$, $\chi^2 = 9.08$). The total numbers of neurons tested in each category are shown within bars.

Alexa Fluor 488-conjugated IB4 (Fig. 1*A*), responsiveness to TRPV1 receptor agonist capsaicin (500 nM; Fig. 1*B* and *G*), as well as the MOR agonist, DAMGO (1 $\mu$M, Fig. 1*D* and *E*). Complete current–voltage relationships were also determined in the absence or presence of N/OFQ (data not shown). As previously reported, N/OFQ did not affect the voltage dependence of HVA $I_{Ca}$ (Borgland *et al.* 2001).

In order to demonstrate the voltage dependence of G-protein inhibition of VGCCs by N/OFQ, we used a pre-pulse protocol (data not shown). In these experiments, HVA $I_{Ca}$ was evoked by two test steps to 0 mV, separated by 190 ms. The second test step was preceded by a conditioning step to +120 mV for 70 ms. In the presence of 300 nM N/OFQ, the amplitude evoked by the first test step was less than the amplitude evoked by the second test step that followed the conditioning step, due to the voltage-dependent relief of G-protein inhibition. This voltage-dependent relief was also previously observed in trigeminal ganglion neurons (Borgland *et al.* 2001). In all subsequent experiments, peak HVA $I_{Ca}$ was elicited by a single depolarising step from –80 mV to 0 mV. A subpopulation of DRG neurons not labelled by IB4 was found to be highly responsive to both N/OFQ and DAMGO. This was correlated strongly with the soma diameter as discussed in detail below.

## N/OFQ selectively inhibits HVA $I_{Ca}$ in a subpopulation of small IB4-negative (peptidergic) DRG neurons

Neurons were defined as N/OFQ sensitive if they showed a reversible inhibition of HVA $I_{Ca}$ of greater than 10% when exposed to maximally effective concentrations of N/OFQ (300 nM) (Fig. 1*C* and *E*). Since size is a good indicator of function in DRG neurons, cells were categorised into three groups based on soma diameter as follows: <20 $\mu$m (small), 20–30 $\mu$m (medium) and >30 $\mu$m (large). In all three groups, neither TRPV1-positive nor -negative neurons emerged as N/OFQ-responsive populations (Fig. 1*G*). Responsiveness to N/OFQ was greatest among small neurons, with 71% of neurons (27 out of 38) displaying inhibition of $I_{Ca}$ greater than 10%, followed by 39% of medium-sized (17 out of 44) then 24% of large (4 out of 17) neurons ($\chi^2 = 13.70$, $P = 0.001$). Most neurons that responded to N/OFQ also responded to the MOR agonist, DAMGO (1 $\mu$M, Fig. 1*D* and *E*).

Responsiveness to N/OFQ in the three neuronal size categories was then examined on the basis of IB4 binding ($IB4^+$ or $IB4^-$; Fig. 1*F*), responsiveness to capsaicin ($TRPV1^+$ or $TRPV1^-$; Fig. 1*G*) and DAMGO. Responsiveness to N/OFQ was enriched in small IB4-negative neurons. N/OFQ (300 nM) produced 51 ± 3% inhibition of HVA $I_{Ca}$ in 85% (17 out of 20) of small-diameter (<20 $\mu$m) IB4 neurons (Fig. 2*B*). Furthermore, 88% (15 out of 17) of small neurons that responded to N/OFQ were also responsive to DAMGO although DAMGO usually produced less inhibition of HVA $I_{Ca}$ than N/OFQ (34 ± 4%, $n = 15$) in this population of neurons (Fig. 2*B*). The native peptide agonist [$Met^5$]-enkephalin (10 $\mu$M) produced similar inhibition to that produced by DAMGO (data not shown). This group of small, presumed peptidergic neurons was thus identified as a distinct population of DRG neurons highly responsive to both N/OFQ and DAMGO. In contrast to the N/OFQ-responsive population of small, presumed peptidergic neurons, N/OFQ inhibited HVA $I_{Ca}$ in only 30% (3 out of 10) of small $IB4^+$ neurons (Fig. 2). All three of these responsive small $IB4^+$ neurons also responded to DAMGO. In neurons >20 $\mu$m diameter, there was no distinct correlation between IB4 binding and response to N/OFQ, perhaps because very few medium- to large-sized neurons were $IB4^+$ (6 out of 47), as reported elsewhere (Gerke & Plenderleith, 2001). Responses to capsaicin did not distinguish responses to N/OFQ for any size DRG neurons. Similar proportions of N/OFQ-responsive neurons were found among $TRPV1^+$ and $TRPV1^-$ neurons of all sizes (Fig. 1*G*).

## ORL1R desensitization is not correlated with a decrease in N-type $I_{Ca}$

Experiments to investigate whether or not prolonged application of a supramaximal concentration of N/OFQ reduced surface expression of the N-type VGCCs were carried out in DRG neurons that were less than 20 $\mu$m diameter and did not exhibit IB4 binding. Application of increasing concentrations of N/OFQ to this subpopulation of DRG neurons produced a maximal effect at concentrations between 30 and 100 nM (Fig. 3*A*); 300 nM N/OFQ was therefore considered supramaximal. Ω-Conotoxin CVID (CVID) is a highly selective antagonist of N-type VGCCs (Lewis *et al.* 2012). Internalization of $Ca_v2.2$ channels, if it occurs during desensitization of the ORL1R, should be reflected as a reduction in the proportion of HVA $I_{Ca}$ sensitive to inhibition by a maximal concentration of CVID. As shown in Fig. 3*B*, a concentration of 300 nM of CVID was sufficient to produce maximal inhibition.

ORL1R desensitisation was determined in small, IB4-negative DRG neurons during prolonged exposure (10 min) to a supramaximal concentration of N/OFQ (300 nM). Desensitization was measured both by the decline in response to the supramaximal concentration as well as the response to a submaximal, probe concentration of N/OFQ before and after the 10 min application of 300 nM N/OFQ. As previously discussed for desensitization of MOR in neurons, the decline in response

to a submaximal concentration of agonist provides a sensitive index of desensitization (Connor *et al.* 2004).

Pronounced ORL1 desensitization occurred in all neurons tested (Fig. 4*A*), when measured either as the decline in response to the supramaximal, or the submaximal, probe concentration of N/OFQ. The amplitude of inhibition by 300 nM N/OFQ decreased significantly from 44 ± 3% initially to 25 ± 2% after 10 min ($n = 5$, $P = 0.0004$, paired $t$ test). Inhibition of HVA $I_{Ca}$ by 10 nM N/OFQ also decreased significantly from 28 ± 6% to 7 ± 2% ($P = 0.006$). These results suggest that exposure to a supramaximal concentration of N/OFQ for 10 min

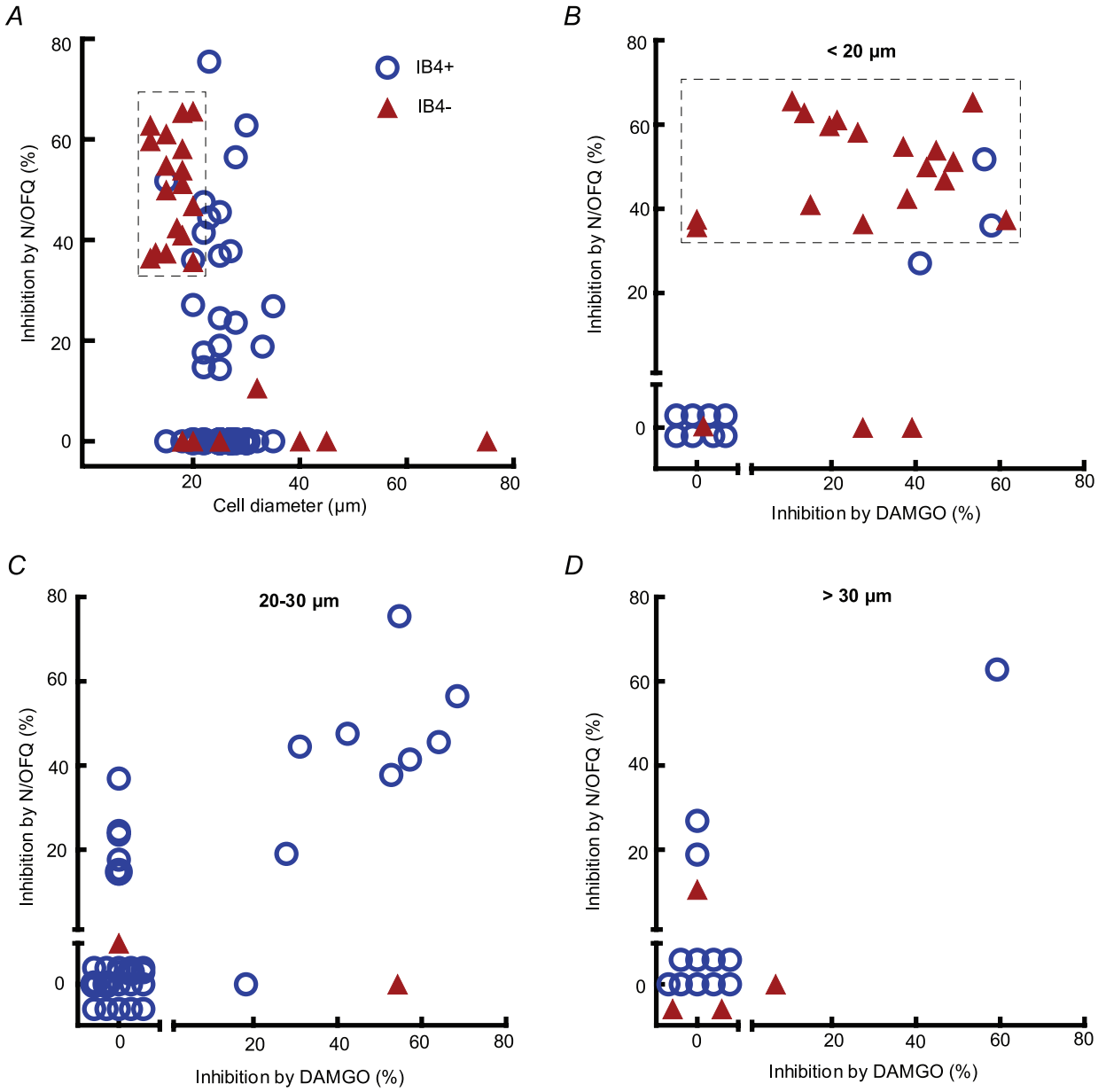


**Figure 2. Inhibition of HVA $I_{Ca}$ by N/OFQ and DAMGO in IB4-positive and negative DRG neurons**
*A*, scatter-plot of soma size *versus* percentage of inhibition of HVA $I_{Ca}$ by N/OFQ. Most N/OFQ-responsive neurons were smaller than 30 $\mu$m. Both IB4$^+$ and IB4$^-$ cells showed a response to N/OFQ overall. As highlighted by the box, responsiveness to N/OFQ was concentrated in small IB4$^-$ neurons. *B*, scatter-plot showing percentage of HVA $I_{Ca}$ inhibition by DAMGO *versus* N/OFQ for neurons smaller than 20 $\mu$m. As highlighted by the box, almost all IB4$^-$ neurons responded to both N/OFQ and DAMGO compared with IB4$^+$ neurons. Subsequent experiments in this study were performed on this population. *C* and *D*, scatter-plot showing percentage of HVA $I_{Ca}$ inhibition by DAMGO *versus* N/OFQ for neurons between 20 to 30 $\mu$m diameter and greater than 30 $\mu$m, respectively. No distinct N/OFQ-responsive subpopulation was seen in these groups.

produces regulation (desensitization) of ORL1R function under our recording conditions.

Although ORL1R desensitization was readily observed, exposure of small, IB4-negative DRG neurons to a supramaximal concentration of N/OFQ (300 nM) for 10 min affected neither overall HVA $I_{Ca}$ density nor the proportion of N-type channels susceptible to inhibition by CVID. To control for rundown of HVA $I_{Ca}$, recordings were made for a similar duration in control neurons (20–30 min) before applying 300 nM CVID. Over the total duration of recording prior to application of CVID, similar rundown was observed in N/OFQ-exposed ($87 \pm 5.5\%$ of initial $I_{Ca}$, $n = 5$) and control ($88 \pm 7\%$ of initial $I_{Ca}$, $n = 5$) neurons. The duration of recordings over which rundown was determined did not differ between groups ($25.1 \pm 1.6$ min, $n = 5$ for control, $25.7 \pm 2$ min, $n = 5$ for N/OFQ-exposed). In the same group of neurons, HVA $I_{Ca}$ density was not significantly affected after washout from 10 min exposure to N/OFQ ($127 \pm 24$ pA pF$^{-1}$ in treated *versus* $172 \pm 39$ pA pF$^{-1}$ in control neurons; $P = 0.36$). There was also no significant difference in the proportion of HVA $I_{Ca}$ susceptible to inhibition by CVID (Fig. 4*B*).

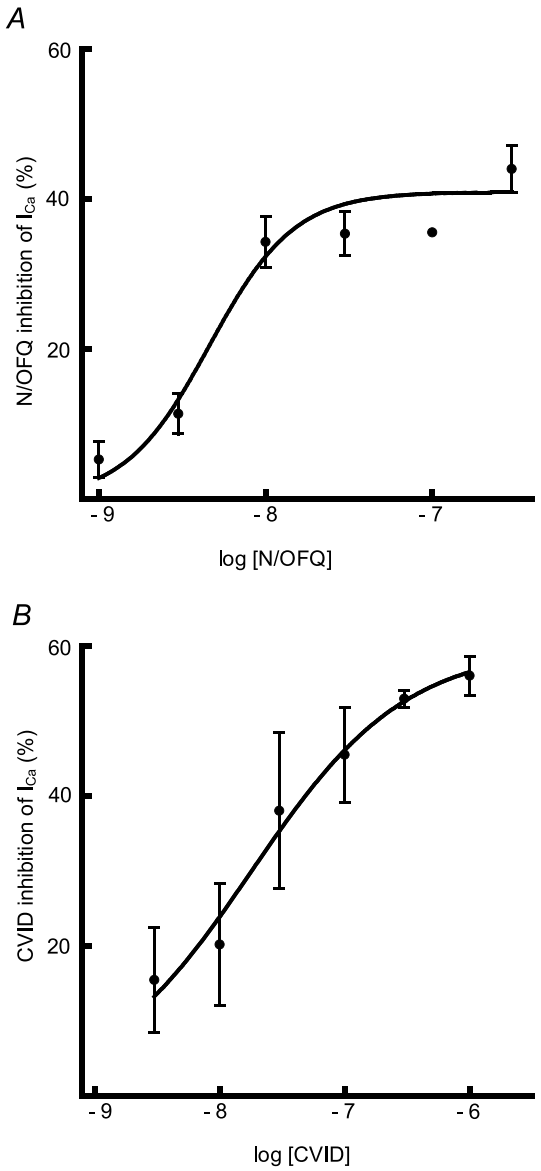


**Figure 3. Concentration–response curves**
Concentration–response curves for *A*, N/OFQ and *B*, CVID in IB4$^-$ neurons smaller than 20 $\mu$m ($n = 3$–10 cells per data point). Maximal effects were observed at 300 nM for both N/OFQ and CVID, which was the concentration used in the subsequent experiments.

## Prolonged incubation with N/OFQ or N/OFQ plus met-enkephalin did not decrease N-type HVA $I_{Ca}$

The failure to observe a reduction in N-type HVA $I_{Ca}$ during whole-cell patch-clamp recordings might have been due to incubation temperature (22–24°C), duration of N/OFQ exposure (10 min) or the whole-cell procedure *per se*. To test this, DRG neurons were incubated at 37°C with either N/OFQ (300 nM) or N/OFQ (300 nM) plus met-enkephalin (ME, 10 $\mu$M) for 30 min immediately prior to patch-clamp recording. Following incubation, the culture dishes containing the neurons were perfused with HBS at room temperature for 5 min before recordings were made. HVA $I_{Ca}$ density and susceptibility to inhibition by CVID was then used to determine the proportion of N-type currents. Control neurons were incubated at 37°C for 30 min in the absence of either agonist. Incubation in N/OFQ or N/OFQ plus ME did not reduce HVA $I_{Ca}$ density, which was $112 \pm 11$ ($n = 16$), $133 \pm 9$ ($n = 13$) and $174 \pm 27$ ($n = 6$) pA pF$^{-1}$ in control, N/OFQ- and N/OFQ plus ME-exposed neurons, respectively. If anything there was a small increase in HVA $I_{Ca}$ density in cells exposed to N/OFQ plus ME ($P = 0.02$, Dunnett's *post hoc* test). There was also no decrease in the proportion of HVA $I_{Ca}$ susceptible to inhibition by CVID (Fig. 4*C*). Therefore, prolonged incubation with ORL1R or MOR agonists did not produce any decrease in the N-type HVA $I_{Ca}$ in rat DRG neurons.

## Incubation with N/OFQ does not reduce the contribution of N-type HVA $I_{Ca}$ to primary afferent synapses in spinal dorsal horn

Calcium influx through N-type VGCCs contributes substantially to neurotransmitter release at primary afferent synapses in the spinal cord dorsal horn (Heinke *et al.* 2004; Rycroft *et al.* 2007) and N/OFQ directly inhibits neurotransmitter release at the same synapses, at least partly via inhibition of N-type HVA $I_{Ca}$ (Liebel *et al.* 1997). The possibility that N/OFQ down-regulates $Ca_v2.2$ on primary afferent synapses was therefore examined in spinal cord slices. As reported elsewhere (Liebel *et al.* 1997), N/OFQ

(10 $\mu$M) reduced the primary afferent eEPSC amplitude in all neurons tested (Fig. 5*A*). Higher concentrations of both N/OFQ and CVID were used in the slice experiments in order to compensate for peptidase activity, as previously reported in spinal tissue (Suder *et al.* 1999). Interestingly, the inhibitory effect of N/OFQ was significantly larger in lamina I neurons where peptidergic afferents (IB4-negative) predominantly terminate (Braz *et al.* 2005) compared with lamina $II_{inner}$ neurons where IB4-positive fibres terminate ($P = 0.025$).

Spinal cord slices were then incubated at 37°C with N/OFQ (10 $\mu$M) or ACSF for 30 min to determine whether activation of ORL1Rs in primary afferent nerve terminals could internalize $Ca_v2.2$. After washout of N/OFQ for at least 20 min the effect of CVID (1 $\mu$M) on eEPSCs was determined (Fig. 5*B*). There was no significant difference in the effect of CVID on evoked EPSC amplitude in spinal cord slices incubated with N/OFQ compared with those incubated with vehicle (Fig. 5*C*) in either lamina I or lamina $II_{inner}$.

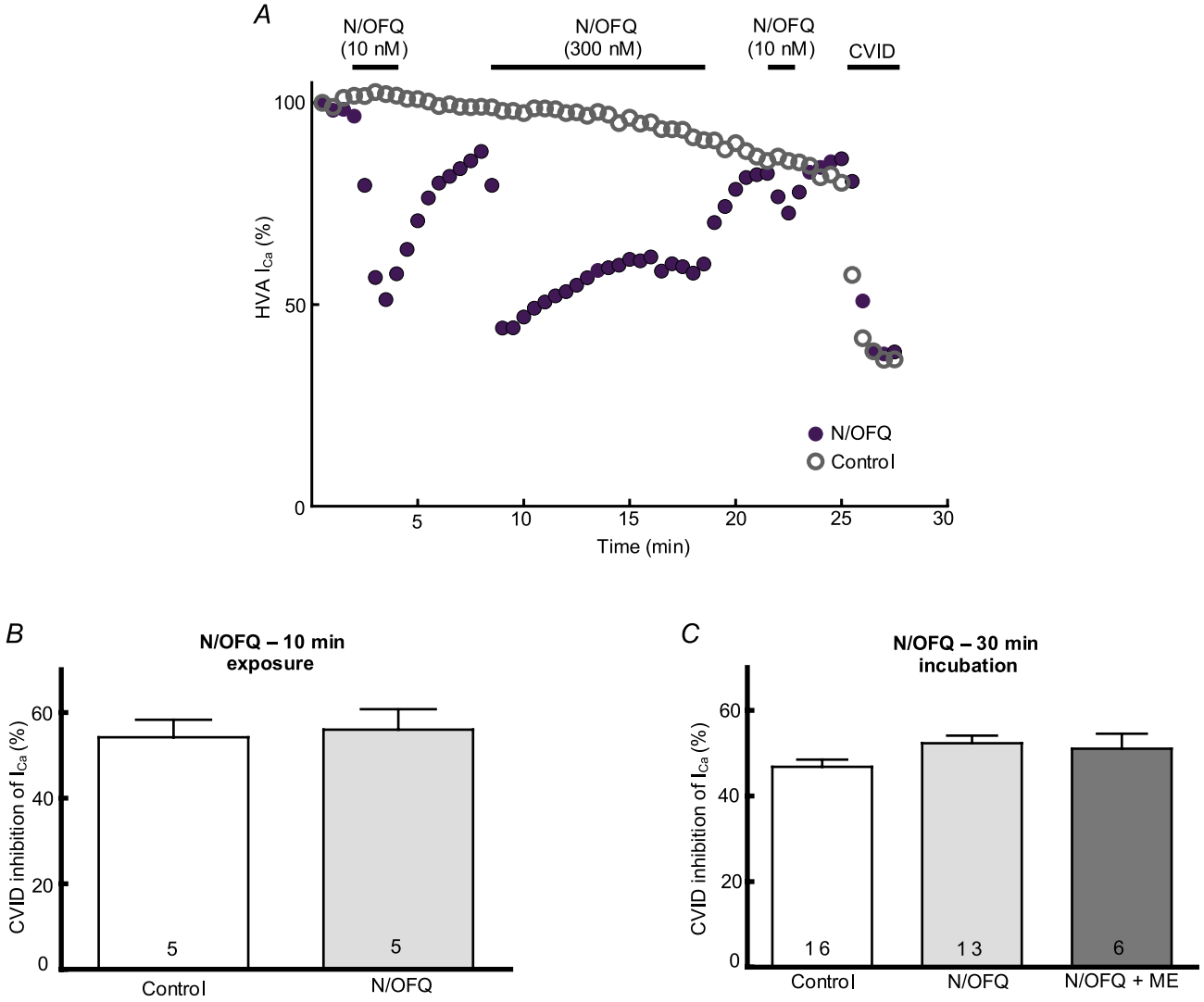


**Figure 4. Effects of prolonged exposure to N/OFQ on N-type HVA $I_{Ca}$ in IB4-negative DRG neurons**
*A*, representative time plot of ORL1R desensitisation in IB4$^-$ DRG neurons smaller than 20 $\mu$m. 10 nM N/OFQ was used as a probe concentration and 300 nM N/OFQ as a supramaximal desensitising concentration. Note the attenuated response to the probe concentration following a 10 min exposure to 300 nM N/OFQ. Following recovery of $I_{Ca}$ after washout of N/OFQ, 300 nM CVID was applied to measure the proportion of N-type current. A representative time plot from a neuron not exposed to N/OFQ is also shown. Note that the rundown in $I_{Ca}$ is comparable in both cells. N-type $I_{Ca}$ proportions measured using 300 nM CVID are also very similar in both cells. *B*, no change was observed in the proportion of N-type current in IB4$^-$ neurons smaller than 20 $\mu$m following desensitisation of ORL1R in response to 10 min agonist exposure. *C*, no change was observed in the proportion of N-type current in IB4$^-$ neurons smaller than 20 $\mu$m following incubation at 37°C for 30 min with vehicle, N/OFQ (300 nM) or both N/OFQ and [Met$^5$]-enkephalin (ME, 10 $\mu$M).

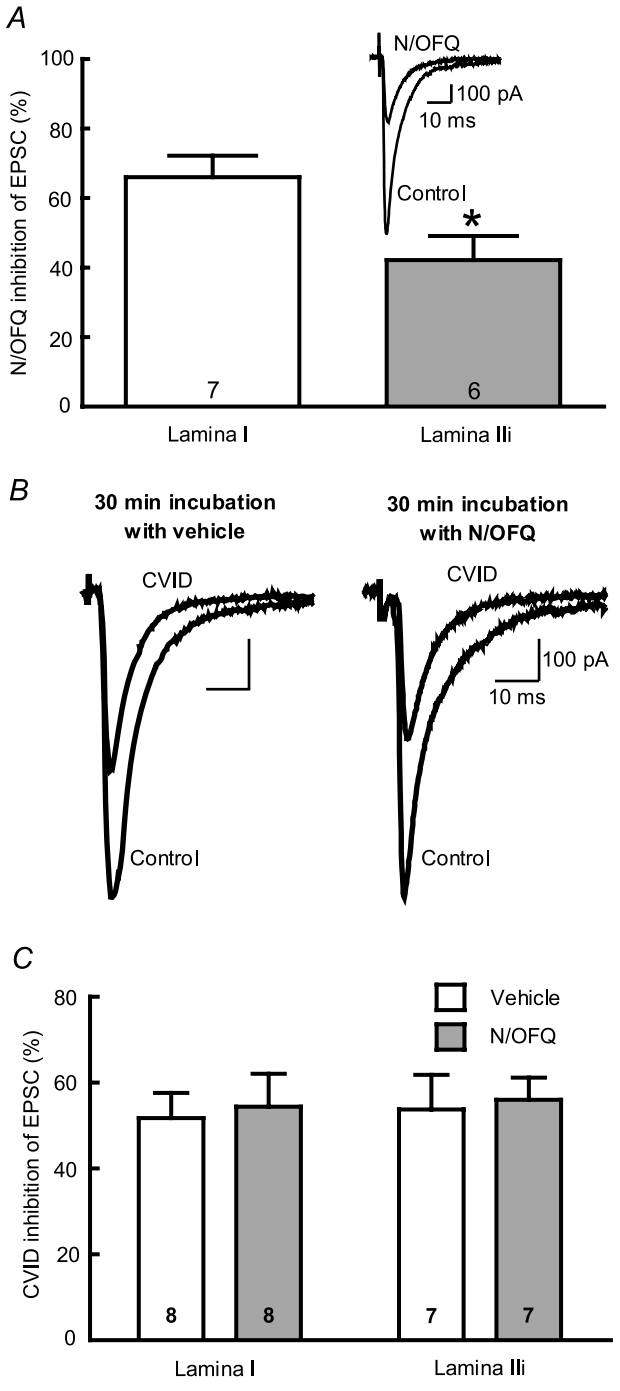


**Figure 5. Effects of prolonged exposure to N/OFQ on primary afferent eEPSCs in dorsal horn of the spinal cord**
*A*, percentage of inhibition of evoked EPSCs by N/OFQ (1 $\mu$M). A significantly higher inhibition was observed in lamina I neurons compared with lamina $II_{inner}$ ($P = 0.025$). Inset, representative trace showing inhibition of an evoked EPSC in the dorsal horn by N/OFQ (1 $\mu$M). *B*, representative traces showing inhibition of evoked EPSCs by CVID (1 $\mu$M) following a 30 min incubation with vehicle or N/OFQ (10 $\mu$M). *C*, percentage of inhibition of evoked EPSCs by CVID (1 $\mu$M). No significant difference was seen between EPSCs recorded from lamina I and lamina $II_{inner}$. Further, incubating the slices with N/OFQ (10 $\mu$M) for 30 min prior to recording did not affect the inhibition of EPSC amplitude by CVID.

## Discussion

This study has characterised a distinct subpopulation of rat sensory neurons that is highly responsive to N/OFQ and MOR agonists, and is IB4-negative and smaller than 20 $\mu$m in diameter. A large proportion of these neurons presumably represents small nociceptive peptidergic sensory neurons (e.g. Kitchener *et al.* 1993; Gerke & Plenderleith, 2001). Previous studies have reported varied distribution of ORL1R in sensory neurons. An *in situ* hybridisation study reported ORL1R mRNA expression in medium to large rat DRG neurons (Pettersson *et al.* 2002). Immunohistochemical studies in rat have reported enrichment of ORL1R-like immunoreactivity in small- to medium-sized DRG neurons (Chen & Sommer, 2006) or have found little selective localization at all (Monteillet-Agius *et al.* 1998; Altier *et al.* 2006). Previous physiological studies have also reported modest enrichment of responsiveness to N/OFQ in small- to medium-sized rat DRG neurons (Beedle *et al.* 2004) and similar enrichment was found in small mouse trigeminal ganglion neurons (Borgland *et al.* 2001). It is unlikely that the pre-incubation of isolated DRG neurons in IB4 affected the classification of subtypes because this procedure has been reported to have no effect on calcium currents or the actions of opioids on labelled DRG neurons (Wu & Pan, 2004; Wu *et al.* 2004).

The present identification of a subpopulation of small IB4-negative DRG neurons highly responsive to N/OFQ is of interest because the role of ORL1R in nociceptive and sensory processing remains unclear (Zeilhofer & Calò, 2003; Lambert, 2008). It has previously been reported that peptidergic and non-peptidergic neurons are involved in parallel pain pathways (Braz *et al.* 2005). IB4-positive neurons were found to be nociceptive and project preferentially to lamina $II_{inner}$ of the dorsal horn, whilst IB4-negative neurons were found to synapse onto lamina I projection neurons (Kitchener *et al.* 1993; Gerke & Plenderleith, 2001). These two regions of the spinal cord then project to different supraspinal regions involved in processing pain (Braz *et al.* 2005). Furthermore, these two populations of neurons receive sensory information preferentially from different targets; IB4-positive neurons receive mostly cutaneous input and peptidergic, IB4-negative neurons predominantly innervate muscle and *vice versa* (Plenderleith & Snow, 1993; Wang *et al.* 1998). The present findings therefore suggest a preferential role of the ORL1R-N/OFQ system in peptidergic sensory pathways. This is supported by the findings of significantly greater inhibition of eEPSCs by N/OFQ in lamina I, which is preferentially innervated by peptidergic (IB4-negative) primary afferent fibres than lamina $II_{inner}$ where IB4-positive fibres preferentially terminate (Kitchener *et al.* 1993; Braz *et al.* 2005).

By identifying a highly selective subpopulation of DRG neurons with >80% of cells highly responsive to N/OFQ, it was possible to test whether activation of this receptor down-regulates $Ca_v2.2$ in native neurons as has been reported in cultured cells (Altier *et al.* 2006; Evans *et al.* 2010). This was achieved by direct measurement of HVA $I_{Ca}$ density in small, IB4-negative DRG neurons, as well sensitivity to the highly selective N-type VGCC blocker, CVID in these neurons and primary afferent terminals (Lewis *et al.* 2000, 2012; Rycroft *et al.* 2007). Although many previous studies have used $\omega$-conotoxins GVIA or MVIIA as specific N-type VGCC inhibitors, we chose CVID for its higher selectivity for $Ca_v2.2$ than other $\omega$-conotoxins, as well as irreversibility of inhibition (Lewis *et al.* 2000, 2012). Furthermore, our previous study demonstrated a robust and reproducible inhibitory effect of CVID on eEPSCs recorded in spinal cord that did not differ from MVIIA (Rycroft *et al.* 2007). In the present study, no functional evidence was found for internalisation of the N-type VGCC in DRG cell bodies or their nerve terminals in the dorsal horn. Previous studies utilised imaging and electrophysiological techniques in the tsA-201 cell line overexpressing both ORL1 and $Ca_v2.2$ (Altier *et al.* 2006; Evans *et al.* 2010). However, in native DRG neurons, only imaging studies were performed (Altier *et al.* 2006). Inability to test this electrophysiologically was presumably due to the lack of information regarding ORL1R (and MOR) expression in different populations of sensory neurons. The present study has overcome this limitation by developing criteria to select DRG neurons that express highly effective coupling of ORL1 to HVA $I_{Ca}$ in nearly all neurons. Small IB4-negative DRG neurons also express a large proportion of $Ca_v2.2$ (Figs 3 and 4), as reported elsewhwere (Wu & Pan, 2004). Using this approach, no evidence could be found for either a reduced VGCC current density or proportion of N-type channels contributing to HVA $I_{Ca}$ after prolonged exposure to high concentrations of N/OFQ. Although these findings are at odds with the findings of Altier *et al.* (2006) and Evans *et al.* (2010), whole-cell patch-clamp recording is arguably the most sensitive and reliable method for determing a functional change in surface expression of VGCC current density and, using selective channel toxins, determining changes in VGCC subtypes.

Exposure of small IB4-negative DRG neurons to a supramaximal concentration of N/OFQ while continuously monitoring HVA $I_{Ca}$ at room temperature could be criticized because the experiment was performed for 10 min at room temperature, which might inhibit endocytosis. Alternatively or additionally, diffusion of a critical intracellular mediator into the patch pipette could have impaired endocytosis of $Ca_v2.2$.

However, this experiment did establish that exposure to a high concentration of N/OFQ reliably produced functional desensitization of ORL1R, which is closely related to endocytosis for many GPCRs (e.g. Dang & Christie, 2012). It might be expected that recovery of ORL1R function after desensitization would be very prolonged due to endocytosis and recycling or degradation. The time-course for resensitization of ORL1R is unknown but, if it resembles related opioid receptors, would require more than 60 min for complete recovery of function (Dang & Williams, 2004; Dang *et al.* 2011; Quillinan *et al.* 2011) which would not be feasible to study by examining modulation of $I_{Ca}$ in DRG neurons.

These potential limitations would not apply to prolonged (30 min) pre-incubation of DRG neurons at 37°C in N/OFQ or N/OFQ plus met-enkephalin, which also produced no reduction in VGCC current density or proportion of N-type HVA $I_{Ca}$. It is most unlikely that the calcium channel expression was restored during the brief recovery period between termination of pre-incubation in N/OFQ and determination of HVA $I_{Ca}$ current density because Altier *et al.* (2006) reported in tsA cells that endocytosis of $Ca_v2.2$ was followed by targeting for lysosomal degradation of the channel.

This study also found no evidence for down-regulation of $Ca_v2.2$ following prolonged N/OFQ incubation in nerve terminals of DRG neurons in spinal cord slices. This is especially relevant as the N-type VGCC, along with the P/Q-type, is responsible for triggering neurotransmitter release and is highly localised on DRG nerve terminals found in the dorsal horn of spinal cord (Heinke *et al.* 2004). The proportion of inhibition of primary afferent eEPSCs found here using CVID was also consistent with the inhibition reported using CVID, MVIIA (Rycroft *et al.* 2007) or GVIA at C-fibre afferents (Heinke *et al.* 2004).

It is difficult to reconcile the present findings with those of Altier *et al.* (2006), particularly in DRG neurons. It is possible that endocytosis and down-regulation of $Ca_v2.2$ is mediated by activation of ORL1 under our conditions but only in a neuronal subpopulation we did not record from, i.e. IB4- positive or larger neurons. If this is the case, then the internalisation mechanism is not expressed by small peptidergic neurons or any primary afferent nerve terminals. We also cannot rule out the possibility that the internalization mechanism, if present, cannot be detected in acutely isolated neurons and spinal cord slices. However Altier *et al.* (2006) also presented correlative immunohistochemical evidence for $Ca_v2.2$ internalization in acutely isolated DRG neurons, so this is an unlikely reason for the discrepancy. It is also possible, but seems unlikely, that $Ca_v2.2$ internalization and degradation did occur in our experiments but was balanced by an equally increased rate of *de novo* insertion of N-type channels into the surface membrane. A potential control for this in future studies in cell culture might

be prolonged incubation (∼40 h) in gabapentin, which disrupts trafficking of the channel to the membrane (Hendrich *et al.* 2008).

In conclusion, the present study has identified a sub-population of rat small IB4-negative DRG neurons that project to the superficial dorsal horn of the spinal cord and are very responsive to both N/OFQ and opioid agonists. However, no evidence was found for a previously proposed prolonged down-regulation of N-type VGCCs following exposure to high concentrations of N/OFQ in these neurons or their central nerve terminals in spinal cord slices. Down-regulation of N-type VGCCs following exposure to high concentrations of N/OFQ therefore appears to be of no physiological significance in native sensory neurons.

## References


Altier C, Khosravani H, Evans RM, Hameed S, Peloquin JB, Vartian BA *et al.* (2006). ORL1 receptor-mediated internalization of N-type calcium channels. *Nat Neurosci* **9**, 31–40.

Beedle AM, McRory JE, Poirot O, Doering CJ, Altier C, Barrere C *et al.* (2004). Agonist-independent modulation of N-type calcium channels by ORL1 receptors. *Nat Neurosci* **7**, 118–125.

Borgland SL, Connor M & Christie MJ (2001). Nociceptin inhibits calcium channel currents in a subpopulation of small nociceptive trigeminal ganglion neurons in mouse. *J Physiol* **536**, 35–47.

Braz JM, Nassar MA, Wood JN & Basbaum AI (2005). Parallel 'pain' pathways arise from subpopulations of primary afferent nociceptor. *Neuron* **47**, 787–793.

Chen Y & Sommer C (2006). Nociceptin and its receptor in rat dorsal root ganglion neurons in neuropathic and inflammatory pain models: implications on pain processing. *J Peripher Nerv Syst* **11**, 232–240.

Chen Y & Sommer C (2007). Activation of the nociceptin opioid system in rat sensory neurons produces antinociceptive effects in inflammatory pain: involvement of inflammatory mediators. *J Neurosci Res* **85**, 1478–1488.

Connor M, Osborne PB & Christie MJ (2004). Mu-opioid receptor desensitization: is morphine different? *Br J Pharmacol* **143**, 685–696.

Connor M, Vaughan CW, Chieng B & Christie MJ (1996*a*). Nociceptin receptor coupling to a potassium conductance in rat locus coeruleus neurones *in vitro*. *Br J Pharmacol* **119**, 1614–1618.

Connor M, Yeo A & Henderson G (1996*b*). The effect of nociceptin on $Ca^{2+}$ channel current and intracellular $Ca^{2+}$ in the SH-SY5Y human neuroblastoma cell line. *Br J Pharmacol* **118**, 205–207.

Corbani M, Gonindard C & Meunier JC (2004). Ligand-regulated internalization of the opioid receptor-like 1: a confocal study. *Endocrinology* **145**, 2876–2885.

Courteix C, Coudore-Civiale MA, Privat AM, Pelissier T, Eschalier A & Fialip J (2004). Evidence for an exclusive antinociceptive effect of nociceptin/orphanin FQ, an endogenous ligand for the ORL1 receptor, in two animal models of neuropathic pain. *Pain* **110**, 236–245.

Dang VC, Chieng B, Azriel Y & Christie MJ (2011). Cellular morphine tolerance produced by $\beta$arrestin-2-dependent impairment of $\mu$-opioid receptor resensitization. *J Neurosci* **31**, 7122–7130.

Dang VC & Christie MJ (2012). Mechanisms of rapid opioid receptor desensitization, resensitization and tolerance in brain neurons. *Br J Pharmacol* **165**, 1704–1716.

Dang VC & Williams JT (2004). Chronic morphine treatment reduces recovery from opioid desensitization. *J Neurosci* **24**, 7699–7706.

Evans RM, You H, Hameed S, Altier C, Mezghrani A, Bourinet E & Zamponi GW (2010). Heterodimerization of ORL1 and opioid receptors and its consequences for N-type calcium channel regulation. *J Biol Chem* **285**, 1032–1040.

Gerke MB & Plenderleith MB (2001). Binding sites for the plant lectin *Bandeiraea simplicifolia* I-isolectin $B_4$ are expressed by nociceptive primary sensory neurones. *Brain Res* **911**, 101–104.

Hayashi S, Nakata E, Morita A, Mizuno K, Yamamura K, Kato A & Ohashi K (2010). Discovery of {1-[4-(2-{hexahydropyrrolo[3,4-c]pyrrol-2(1H)-yl}-1H-benzimidazol-1-yl)pip eridin-1-yl]cyclooctyl}methanol, systemically potent novel non-peptide agonist of nociceptin/orphanin FQ receptor as analgesic for the treatment of neuropathic pain: design, synthesis, and structure-activity relationships. *Bioorg Med Chem* **18**, 7675–7699.

Heinke B, Balzer E & Sandkühler J (2004). Pre- and postsynaptic contributions of voltage-dependent $Ca^{2+}$ channels to nociceptive transmission in rat spinal lamina I neurons. *Eur J Neurosci* **19**, 103–111.

Hendrich J, Van Minh AT, Heblich F, Nieto-Rostro M, Watschinger K, Striessnig J *et al.* (2008). Pharmacological disruption of calcium channel trafficking by the a2d ligand gabapentin. *Proc Nat Acad Sci U S A* **105**, 3628–3633.

Kitchener PD, Wilson P & Snow PJ (1993). Selective labelling of primary sensory afferent terminals in lamina II of the dorsal horn by injection of *Bandeiraea simplicifolia* isolectin B4 into peripheral nerves. *Neuroscience* **54**, 545–551.

Lambert DG (2008). The nociceptin/orphanin FQ receptor: a target with broad therapeutic potential. *Nat Rev Drug Discov* **7**, 694–710.

Larsson KP, Olsen UB & Hansen AJ (2000). Nociceptin is a potent inhibitor of N-type $Ca^{2+}$ channels in rat sympathetic ganglion neurons. *Neurosci Lett* **296**, 121–124.

Lewis RJ, Dutertre S, Vetter I & Christie M (2012). Conus venom peptide pharmacology. *Pharmacol Rev* in press.

Lewis RJ, Nielsen KJ, Craik DJ, Loughnan ML, Adams DA, Sharpe IA *et al.* (2000). Novel omega-conotoxins from Conus catus discriminate among neuronal calcium channel subtypes. *J Biol Chem* **275**, 35335–35344.

Liebel JT, Swandulla D & Zeilhofer HU (1997). Modulation of excitatory synaptic transmission by nociceptin in superficial dorsal horn neurones of the neonatal rat spinal cord. *Br J Pharmacol* **121**, 425–432.

Meunier JC, Mollereau C, Toll L, Suaudeau C, Moisand C, Alvinerie P *et al*. (1995). Isolation and structure of the endogenous agonist of opioid receptor-like ORL1 receptor. *Nature* **377**, 532–535.

Monteillet-Agius G, Fein J, Anton B & Evans CJ (1998). ORL-1 and mu opioid receptor antisera label different fibers in areas involved in pain processing. *J Comp Neurol* **399**, 373–383.

Okuda-Ashitaka E, Minami T, Matsumura S, Takeshima H, Reinscheid RK, Civelli O & Ito S (2006). The opioid peptide nociceptin/orphanin FQ mediates prostaglandin E2-induced allodynia, tactile pain associated with nerve injury. *Eur J Neurosci* **23**, 995–1004.

Pettersson LM, Sundler F & Danielsen N (2002). Expression of orphanin FQ/ nociceptin and its receptor in rat peripheral ganglia and spinal cord. *Brain Res* **945**, 266–275.

Plenderleith MB & Snow PJ (1993). The plant lectin *Bandeiraea simplicifolia* I-B4 identifies a subpopulation of small diameter primary sensory neurones which innervate the skin in the rat. *Neurosci Lett* **159**, 17–20.

Quillinan N, Lau EK, Virk M, von Zastrow M & Williams JT (2011). Recovery from $\mu$-opioid receptor desensitization after chronic treatment with morphine and methadone. *J Neurosci* **31**, 4434–4443.

Reinscheid RK, Nothacker HP, Bourson A, Ardati A, Henningsen RA, Bunzow JR *et al*. (1995). Orphanin FQ: a neuropeptide that activates an opioidlike G protein-coupled receptor. *Science* **270**, 792–794.

Reiss D, Wichmann J, Tekeshima H, Kieffer BL & Ouagazzal AM (2008). Effects of nociceptin/orphanin FQ receptor (NOP) agonist, Ro64-6198, on reactivity to acute pain in mice: comparison to morphine. *Eur J Pharmacol* **579**, 141–148.

Rycroft BK, Vikman KS & Christie MJ (2007). Inflammation reduces the contribution of N-type calcium channels to primary afferent synaptic transmission onto NK1 receptor-positive lamina I neurons in the rat dorsal horn. *J Physiol* **580**, 883–894.

Spampinato S, Di Toro R, Alessandri M & Murari G (2002). Agonist-induced internalization and desensitization of the human nociceptin receptor expressed in CHO cells. *Cell Mol Life Sci* **59**, 2172–2183.

Spampinato S, Di Toro R & Qasem AR (2001). Nociceptin-induced internalization of the ORL1 receptor in human neuroblastoma cells. *Neuroreport* **12**, 3159–3163.

Suder P, Kotlinska J, Smoluch MT, Sallberg M & Silberring J (1999). Metabolic fate of nociceptin/orphanin FQ in the rat spinal cord and biological activity of its released fragment. *Peptides* **20**, 239–247.

Vikman KS, Rycroft BK & Christie MJ (2008). Switch to $Ca^{2+}$-permeable AMPA and reduced NR2B NMDA receptor-mediated neurotransmission at dorsal horn nociceptive synapses during inflammatory pain in the rat. *J Physiol* **586**, 515–527.

Wang H, Rivero-Melián C, Robertson B & Grant G (1994). Transganglionic transport and binding of the isolectin B4 from *Griffonia simplicifolia* I in rat primary sensory neurons. *Neuroscience* **62**, 539–551.

Wang HF, Robertson B & Grant G (1998). Anterograde transport of horseradish-peroxidase conjugated isolectin B4 from *Griffonia simplicifolia* I in spinal primary sensory neurons of the rat. *Brain Res* **811**, 34–39.

Wu Z-Z, Chen SR & Pan HL (2004). Differential sensitivity of N- and P/Q-type $Ca^{2+}$ channel currents to a mu opioid in isolectin B4-positive and -negative dorsal root ganglion neurons. *J Pharmacol Exp Ther* **311**, 939–947.

Wu Z-Z & Pan HL (2004). High voltage-activated $Ca^{2+}$ channel currents in isolectin B4-positive and -negative small dorsal root ganglion neurons of rats. *Neurosci Lett* **368**, 96–101.

Yamamoto T, Nozaki-Taguchi N & Kimura S (1997). Analgesic effect of intrathecally administered nociceptin, an opioid receptor-like1 receptor agonist, in the rat formalin test. *Neuroscience* **81**, 249–254.

Zeilhofer HU & Calò G (2003). Nociceptin/orphanin FQ and its receptor–potential targets for pain therapy? *J Pharmacol Exp Ther* **306**, 423–429.

## Author contributions

S.S.M. designed and performed the DRG experiments, analysed and interpreted the data, drafted the manuscript and revised it critically for important intellectual content, I.A.N. and B.K.R. performed and analysed spinal cord experiments, M.J.C. contributed to conception, design and analysis of the experiments, drafting the article and revising it critically for important intellectual content. All authors approved the final version.

## Acknowledgements

This study was supported by National Health and Medical Research Council of Australia (NH & MRC). M.J.C. is a NH & MRC Senior Principal Research Fellow (511914). Donation of $\omega$-conotoxin CVID by Professor Richard J Lewis, University of Queensland is gratefully acknowledged. Advice from Professor Mark Connor on DRG dissociation and recording is gratefully acknowledged.